Heat Transfer in Nanostructures for Solid-State Energy Conversion

G. Chen
Assoc. Prof. Mem. ASME
Mechanical Engineering Department,
Massachusetts Institute of Technology,
Cambridge, MA 02139

A. Shakouri
Jack Baskin School of Engineering,
University of California,
Santa Cruz, CA 95064-1077

Solid-state energy conversion technologies such as thermoelectric and thermionic refrigeration and power generation require materials with low thermal conductivity but good electrical conductivity and Seebeck coefficient, which are difficult to realize in bulk semiconductors. Nanostructures such as superlattices, quantum wires, and quantum dots provide alternative approaches to improve the solid-state energy conversion efficiency through size and interface effects on the electron and phonon transport. In this review, we discuss recent research and progress using nanostructures for solid-state energy conversion. The emphasis is placed on fundamental issues that distinguish energy transport and conversion between nanoscale and macroscale, as well as heat transfer issues related to device development and property characterization. [DOI: 10.1115/1.1448331]

Keywords: Conduction, Energy Conversion, Heat Transfer, Microscale Microstructures, Nanoscale, Thermoelectric, Thin Films

1 Introduction

Accompanying the motion of charges in conductors or semiconductors, there is also an associated energy transport. Consider a current flowing through a pair of *n*-type and *p*-type semiconductors connected in series as shown in Fig. 1(*a*). The electrons in the *n*-type material and the holes in the *p*-type material all carry heat away from the top metal-semiconductor junctions, which leads to a cooling at the junctions called the Peltier effect. Conversely, if a temperature difference is maintained between the two ends of the materials as shown in Fig. 1(*b*), higher thermal energy electrons and holes will diffuse to the cold side, creating a potential difference that can be used to power an external load. This Seebeck effect is the principle for thermocouples. For each material, the cooling effect is gauged by the Peltier coefficient Π that relates the heat carried by the charges to the electrical current through $Q=\Pi\times I$. The power generation is measured by the Seebeck coefficient S, which relates the voltage generated to the temperature difference through $\Delta V=-S\times\Delta T$. The Peltier and the Seebeck coefficients are related through the Kelvin relation $\Pi=ST$. Practical devices are made of multiple pairs of *p*-type and *n*-type semiconductors as shown in Fig. 1(*c*). Analysis shows that efficient coolers and power generators should have a large figure-of-merit [1],

$$Z=\frac{\sigma S^2}{k},$$

where σ is the electrical conductivity and k the thermal conductivity. The reason that the electrical conductivity σ enters Z is due to the Joule heating in the element. Naturally, the Joule heat should be minimized by increasing the electrical conductivity. The thermal conductivity k appears in the denominator of Z because the thermoelectric elements also act as the thermal insulation between the hot and the cold sides. A high thermal conductivity causes too much heat leakage through heat conduction. Because Z has a unit of inverse temperature, the nondimensional figure of merit ZT is often used. The best ZT materials are found in semiconductors [2]. Insulators have poor electrical conductivity. Metals have relatively low Seebeck coefficients. In addition, the thermal conductivity of a metal, which is dominated by electrons, is proportional to the electrical conductivity, as dictated by the Wiedemann-Franz law. It is thus hard to realize high ZT in metals. In semiconductors, the thermal conductivity consists of contributions from electrons (k_e) and phonons (k_p), with the majority contribution coming from phonons. The phonon thermal conductivity can be reduced without causing too much reduction in the electrical conductivity. A proven approach to reduce the phonon thermal conductivity is through alloying [3]. The mass difference scattering in an alloy reduces the lattice thermal conductivity significantly without much degradation to the electrical conductivity. The traditional cooling materials are alloys of Bi_2Te_3 with Sb_2Te_3 (such as $Bi_{0.5}Sb_{1.5}Te_3$, *p*-type) and Bi_2Te_3 with Bi_2Se_3 (such as $Bi_2Te_{2.7}Se_{0.3}$, *n*-type), with a ZT at room temperature approximately equals to one [2]. A typical power generation material is the alloy of silicon and germanium, with a $ZT\sim0.6$ at 700°C. Figure 2 plots the theoretical coefficient of performance (COP) and efficiency of thermoelectric coolers and power generators for different ZT values. Also marked in the figures for comparison are other cooling and power generation technologies. Materials with $ZT\sim1$ are not competitive against the conventional fluid-based cooling and power generation technologies. Thus, solid-state cooler and power generators have only found applications in niche areas, such as cooling of semiconductor lasers and power generation for deep space exploration, although the application areas have been steadily increasing.

While the search for high ZT materials before 1990s have been mostly limited to bulk materials, there has been extensive research in the area of artificial semiconductor structures in the last 30 years for electronic and optoelectronic applications. Various means of producing ultrathin and high quality crystalline layers (such as molecular beam epitaxy and metalorganic chemical vapor deposition) have been used to alter the ''bulk'' characteristics of the materials. Drastic changes are produced by changing the crystal periodicity (by e.g., depositing alternating layers of different crystals), or by changing the electron dimensionality (by confining the carriers in a plane (quantum well) or in a line (quantum wire, etc.)). Even though electrical and optical properties of these artificial crystalline structures have been extensively studied, much less attention has been paid to their thermal and thermoelectric properties. Thermoelectric properties of low-dimensional structures started to attract attention in the 1990s, in parallel to renewed interests in certain bulk thermoelectric materials such as skutterudites [4]. Compared to the research in bulk materials that emphasizes reducing the thermal conductivity, nanostructures offer the chance of improving both the electron and phonon transport through the use of quantum and classical size and interface effects. Several directions have been explored such as quantum size effects for electrons [5,6], thermionic emission at interfaces [7,8], and interface scattering of phonons [9,10]. Impressive ZT values have been reported in some low-dimensional structures [11,12]. Comprehensive reviews on the progress of thermoelectric

Contributed by the Heat Transfer Division for publication in the JOURNAL OF HEAT TRANSFER. Manuscript received by the Heat Transfer Division July 24, 2001; revision received November 20, 2001. Editor: V. K. Dhir.

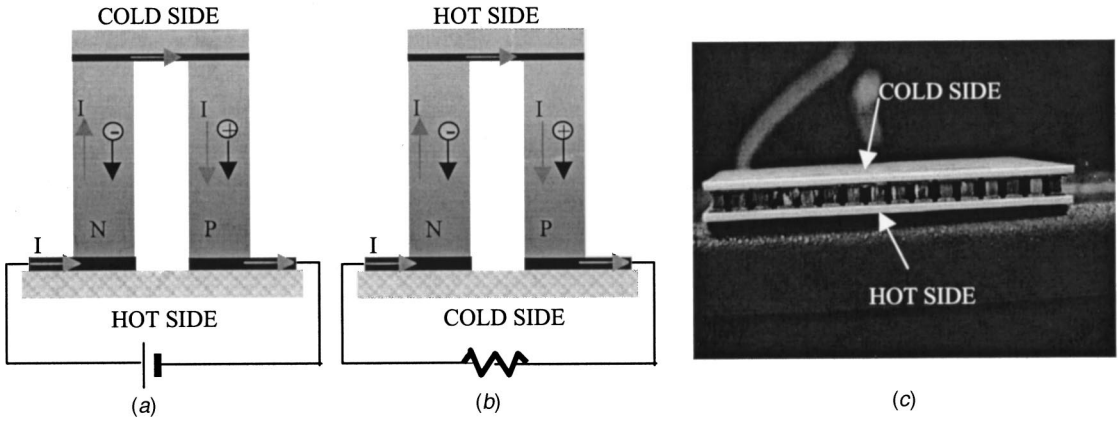

Fig. 1 Illustration of thermoelectric devices (*a*) cooler, (*b*) power generator, and (*c*) an actual device

materials research is presented in a recently published series [4] and in the proceedings of the various international conferences on thermoelectrics held in recent years.

In this article, we have in mind readers interested in nano- and microscale heat transfer and energy conversion and focus on thermoelectric energy conversion in low-dimensional structures. The emphasis is placed on fundamental issues that distinguish energy transport and conversion between nanoscale and macroscale, as well as heat transfer issues related to device development and property characterization. One of our aims is to provide the readers with an overview of recent developments. Because of the wide scope of work being carried out, the cited references are far from complete. Along with the review, we hope to stimulate the readers by pointing out unsolved, challenging questions related to the theory, characterization, and device development.

2 Formulation of Thermoelectric Effects

In solid-state coolers or power generators, heat is carried by charges from one place to another. The current density and heat flux carried by electrons can be expressed as [13]

$$\mathbf{J}(\mathbf{r}) = \frac{1}{4\pi^3}\int\int\int q\mathbf{v}(\mathbf{k})f(\mathbf{r},\mathbf{k})d^3\mathbf{k} \tag{1}$$

$$\mathbf{J}_Q(\mathbf{r}) = \frac{1}{4\pi^3}\int\int\int [E(\mathbf{k})-E_f(\mathbf{r})]\mathbf{v}(\mathbf{k})f(\mathbf{r},\mathbf{k})d^3\mathbf{k}, \tag{2}$$

where q is the unit charge of each carrier, E_f the Fermi energy, $\mathbf{v}$ the carrier velocity, and the integration is over all the possible wavevectors $\mathbf{k}$ of all the charges. The carrier probability distribution function, $f(\mathbf{r},\mathbf{k})$ is governed by the Boltzmann equation. Considering transport processes occurring much slower than the relaxation process and employing the relaxation time approximation, the Boltzmann equation can be expressed as

$$\mathbf{v}\cdot\nabla_{\mathbf{r}}f + \frac{q\boldsymbol{\varepsilon}}{\hbar}\cdot\nabla_{\mathbf{k}}f = -\frac{f(\mathbf{r},\mathbf{k})-f_{\mathrm{eq}}(\mathbf{r},\mathbf{k})}{\tau(\mathbf{k})}, \tag{3}$$

where is $\boldsymbol{\varepsilon}$ the electric field, $\tau(\mathbf{k})$ the momentum-dependent relaxation time, $\hbar$ the Planck constant divided by 2π, and f_{eq} the equilibrium distribution function. For electrons and holes,

$$f_{\mathrm{eq}}(\mathbf{r},\mathbf{k}) = \frac{1}{1+\exp\left(\dfrac{E(\mathbf{k})-E_f(\mathbf{r})}{k_BT(\mathbf{r})}\right)}, \tag{4}$$

where k_B is the Boltzmann constant, and T the local temperature. Under the further assumption that the local deviation from equilibrium is small, the Boltzmann equation can be linearized and its solution expressed as

$$f(\mathbf{r},\mathbf{k}) = f_{\mathrm{eq}}(\mathbf{r},\mathbf{k}) + \tau(\mathbf{k})\mathbf{v}\left(-\frac{\partial f_{\mathrm{eq}}}{\partial E}\right)\cdot\left[-\frac{E(k)-E_f}{T}\nabla_{\mathbf{r}}T + q\left(\boldsymbol{\varepsilon}-\frac{1}{q}\nabla_{\mathbf{r}}E_f\right)\right]. \tag{5}$$

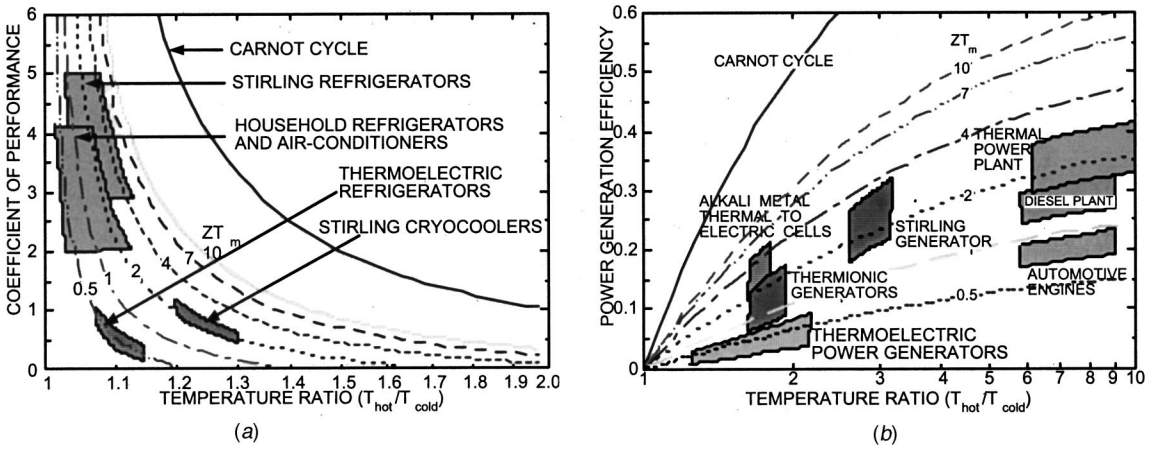

Fig. 2 Comparison of thermoelectric technology with other energy conversion methods for (*a*) cooling and (*b*) power generation

Substituting the above expression in Eqs. (1) and (2) leads to the

$$\mathbf{J}(\mathbf{r})=q^2L_0\left(-\frac{1}{q}\nabla\Phi\right)+\frac{q}{T}L_1(-\nabla T) \tag{6}$$

$$\mathbf{J}_Q(\mathbf{r})=qL_1\left(-\frac{1}{q}\nabla\Phi\right)+\frac{1}{T}L_2(-\nabla_{\mathbf{r}}T), \tag{7}$$

where Φ is the electrochemical potential $(-\nabla\Phi/q=\boldsymbol{\varepsilon}-\nabla E_f/q)$. The transport coefficients L_n are defined by the following integral

$$L_n=\frac{1}{4\pi^3}\int\int\int \tau(\mathbf{k})v(\mathbf{k})v(\mathbf{k})(E(\mathbf{k})-E_F)^n\left(-\frac{\partial f_{\text{eq}}}{\partial E}\right)d^3\mathbf{k}. \tag{8}$$

From the expressions for $\mathbf{J}$ and $\mathbf{J}_Q$, various material parameters such as the electrical conductivity, thermal conductivity due to electrons, and the Seebeck coefficient can be calculated. For simplicity we assume that both the current flow and the temperature gradient are in the *x*-direction:

$$\sigma=J_x/(-\nabla\Phi/q)|_{\nabla_x T=0}=q^2L_0 \tag{9}$$

$$S=(-\nabla\Phi/q)/\nabla_x T|_{J_x=0}=\frac{1}{qT}{L_0}^{-1}L_1 \tag{10}$$

$$k_e=J_{Q_x}/(-\nabla_x T)|_{J_x=0}=\frac{L_2L_0-L_1L_1}{TL_0}. \tag{11}$$

Rewriting the expressions for electrical conductivity and the thermopower in the form of integrals over the electron energy we get

$$\sigma\equiv\int\sigma(E)\left(-\frac{\partial f_{\text{eq}}}{\partial E}\right)dE \tag{12}$$

$$S\equiv\frac{k_B}{q}\frac{\int\sigma(E)\frac{(E-E_F)}{k_BT}\left(-\frac{\partial f_{eq}}{\partial E}\right)dE}{\int\sigma(E)\left(-\frac{\partial f_{eq}}{\partial E}\right)dE}\propto\langle E-E_f\rangle, \tag{13}$$

where we introduced the ''differential'' conductivity,

$$\sigma(E)\equiv q^2\tau(E)\int\int \nu_x^2(E,k_y,k_z)dk_ydk_z\cong q^2\tau(E)\overline{\nu_x^2}(E)D(E), \tag{14}$$

where $D(E)$ is the density of states. $\sigma(E)$ is a measure of the contribution of electrons with energy E to the total conductivity. The Fermi ''window'' factor $(-\partial f_{eq}/\partial E)$ is a bell-shape function centered at $E=E_f$, having a width of $\sim k_BT$. At a finite temperature only electrons near the Fermi surface contribute to the conduction process. In this picture, the thermopower is the ''average'' energy transported by the charge carriers. In order to achieve the best thermoelectric properties, σ (E), within the Fermi window, should be as big as possible, and at the same time, as asymmetric as possible with respect to the Fermi energy.

The thermal conductivity of phonons is also often modeled from the Boltzmann equation under the relaxation time approximation,

$$k_p=\frac{1}{3}\sum\int C(\omega)v_p(\omega)\Lambda(\omega)d\omega, \tag{15}$$

where C is the specific heat of phonons at frequency ω, v_p the phonon group velocity, and Λ the phonon mean free path.

The above formulation for the thermoelectric properties leads to the following possibilities to increase *ZT* and thus the energy conversion efficiency of devices made of nanostructures.

1. Interfaces and boundaries of nanostructures impose constraints on the electron and phonon waves, which lead to a change in their energy states and correspondingly, their density of states and group velocity.
2. The symmetry of the differential conductivity with respect to the Fermi level can be controlled using quantum size effects and classical interface effects (as in thermionic emission).
3. The phonon thermal conductivity can be reduced through interface scattering and through the alteration of the phonon spectrum in low-dimensional structures.

3 Nanostructures for Solid-State Energy Conversion

The transport of electrons and phonons in nanostructures is affected by the presence of the interfaces and surfaces. Since electrons and phonons have both wave and particle characteristics, the transport can fall into two different regimes: totally coherent transport in which electrons or phonons must be treated as waves and totally incoherent transport in which either or both of them can be treated as particles. There is, of course, the intermediate regime where transport is partially coherent—an area that has not been studied extensively. Whether a group of carriers are coherent or incoherent depend on the strength of phase destroying scattering events (such as internal or diffuse interface scattering). In a nanostructure with no phase-destroying scattering events, a monochromatic wave can experience many coherent scatterings while preserving the phase. The coherent superposition of the incoming and scattered waves leads to the formation of new energy bands for electrons and/or phonons. For example, the quantized energy states of electrons in a quantum well are the result of the formation of standing waves inside the structure. The standing wave can be regarded as the superposition of two counter-propagating waves, each experiencing phase preserving reflections at the interfaces. On the other hand, if there is a strong internal scattering (which can be judged from the momentum relaxation time) or if the interface scattering is not phase preserving (such as due to diffuse scattering), no new energy bands form and the energy states of the carriers in such a structure are identical to these in its bulk material. Electron transport in both coherent and incoherent regimes has been considered and potential benefits of nanostructures for the power factor $(S^2\sigma)$ have been studied. Similarly, phonon heat conduction in both regimes has also be considered, although most studies are based on the particle approach. We will divide the discussion into roughly three categories: (1) improving the electronic power factor based on coherent electron states, (2) improving the electronic energy conversion based on interface filtering for incoherent electrons, (3) improving *ZT* by reducing the phonon thermal conductivity.

3.1 Electron Energy States Engineering. This approach was suggested in a pioneering work by Dresselhaus and coworkers [5,6]. The main idea is that energy states in nanostructures are very different from those in macrostructures due to the quantum size effects on electrons. Figure 3 illustrates, qualitatively, the density of states (DOS) of electrons in bulk materials,

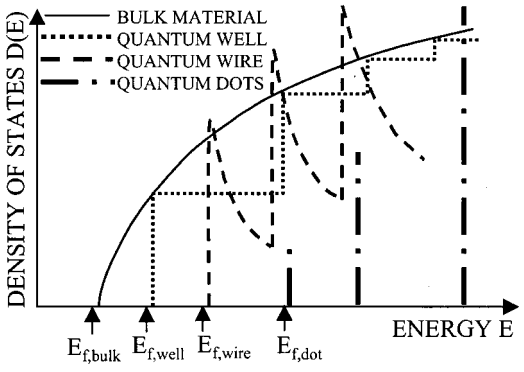

Fig. 3 Schematic illustration of the density-of-states of electrons in bulk, quantum well, quantum wire, and quantum dots materials.

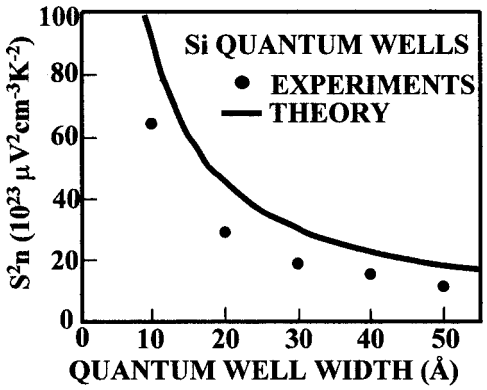

Fig. 4 Product of the Seebeck coefficient square and carrier density as a function of the silicon quantum well width [15]

quantum wells, quantum wires, and quantum dots. Examination of Eq. (13) indicates that the Seebeck coefficient is large when the average electron energy is far apart from the Fermi level. In semiconductors, a large Seebeck coefficient occurs when the Fermi level is inside the band-gap. A Fermi level deep inside the band-gap, however, leads to a low electrical conductivity. The optimized Fermi level usually is close to the band edge. Because the function $\partial f_{eq}/\partial E$ is nonzero only in an energy range $\sim k_B T$ near the Fermi level, the higher the DOS in this range, the larger power factor we can anticipate. In bulk materials, the parabolic shape of the DOS means that the electron density surrounding the Fermi level is small. In quantum structures, the steps and the spikes in the DOS suggest that $S^2\sigma$ can be increased. In a theoretical study by Mahan and Sofo [14], it was suggested that the best thermoelectric materials will have a spike like DOS. Quantum dots fit ideally into such a picture. A single quantum dot, however, is not of much interest for building into useful thermoelectric devices (but may be of interest to create localized cooling on the nanoscale). Thus the study began with quantum wells (extremely thin films) and quantum wires (extremely small wires). Experimental results for transport inside PbTe and Si/SiGe quantum well systems indicated an increase of *ZT* inside the quantum well, as shown in Fig. 4 [15].

A single quantum well, however, cannot be used to build useful devices because the film is too thin (typically less than a few hundreds angstroms). Multilayer structures were therefore used in the proof-of-concept experiments. For multilayer structures such as superlattices, three questions were raised on the effectiveness of the quantum confinement approach [16,17]. One is that electrons will tunnel through the barrier layer when the barriers are very thin. The second argument is that the barrier does not contribute to the thermoelectric transport but does contribute to the reverse heat conduction. And finally, there is also concern of interface scattering of electrons in narrow wells. A possible approach for improving performance is to utilize the quantum confinement effects inside both the quantum well and the barrier layer, and to have electrons in different carrier pockets in momentum space confined in different regions [18,19]. Additionally, the thermal conductivity of very thin superlattices can be reduced due to interface scattering—a topic we will discuss later on [20]. A natural extension of the quantum well and superlattice theory is to quantum wires. Theoretical studies predict a large enhancement of *ZT* inside quantum wires. Experimentally, different quantum wire deposition methods have been explored [6].

The experimental results that are inspired by the theoretical studies have proven to be impressive and unexpected [21]. After the proof-of-concept demonstration of *ZT* enhancement in two-dimensional quantum wells, Harman's group showed that quantum-dot superlattices have a significantly higher power factor than their corresponding bulk materials [22]. Using a thermal conductivity value estimated from bulk properties, *ZT* values as high as two have been reported. At this stage, no models exist to quantitatively explain the observed increase in *ZT*.

The above-discussed approaches are based on transport perpendicular to the confinement directions, i.e., along the film plane or wire axis. There are also considerations of the DOS change for electron transport perpendicular to the film plane of the superlattices [23,24]. These calculations, however, do not show a significant increase of the electronic power factor along these directions and suggest that the thermal conductivity reduction may be a more beneficial factor to explore along this transport direction.

Research for improving *ZT* using quantum confinement of electrons raises several interesting questions related to heat transfer [20]. First, the thermal conductivity along the film plane and wire axis should be reduced due to phonon interface scattering. We will discuss more about this point later. Second, the parasitic thermal conductivity in the barrier layer is still a concern for certain quantum structures that do not utilize the barrier region for electron transport. For example, nanowires can be deposited in an anodized alumina matrix with nanometer scale channels. Although the thermal conductivity of the anodized alumina is relatively small, it is not negligible, and further reduction of the parasitic heat conduction path through such a matrix should be considered [25]. Another very interesting yet little explored aspect is the transport processes in the synthesis of nanowires. Several different methods have been explored, including pressure injection of molten bismuth into the template [26], physical vapor deposition [27], and electrodeposition [28]. Heat and mass transport inside these nanoscale channels could be very different than that in bulk channels. So far, these techniques are developed only through trial-and-error. It is generally found that smaller diameter channels are more difficult to fill, leading to partial filling or discontinuous wires. Systematic studies of the transport processes will help with the optimization of the deposition conditions.

3.2 Heterostructure Integrated Thermionic Refrigeration. Thermionic energy conversion is based on the idea that a high work function cathode in contact with a heat source will emit electrons [29]. These electrons are absorbed by a cold, low work function anode, and they can flow back to the cathode through an external load where they do useful work. Practical vacuum thermionic generators are limited by the work function of available metals or other materials that are used for cathodes. Another important limitation is the space charge effect. The presence of charged electrons in the space between the cathode and anode will create an extra potential barrier between the cathode and anode, which reduces the thermionic current. The materials currently used for cathodes have work functions >0.7 eV, which limits the generator applications to high temperatures >500 K. Mahan [30] proposed these vacuum diodes for thermionic refrigeration. Basically, the same vacuum diodes which are used for generators will work as a cooler on the cathode side and a heat pump on the anode side under an applied bias. Mahan predicted efficiencies of over 80 percent of the Carnot value, but still these refrigerators only work at high temperatures (>500 K). In the following, we will see that heterostructures have a potential to achieve thermionic refrigeration at room temperature [7,31–33]. Vacuum thermionic refrigeration based on resonant tunneling through triangular wells and small gaps in vacuum has been proposed recently [34,35]. Theoretical calculations predict operation at room temperature and below with a cooling power density of 100 W/cm^2. Net cooling based on such vacuum thermionic coolers has yet to be confirmed experimentally.

Using various material systems one can produce different barrier heights in the anode and in the cathode (typically 0 to 0.4 eV). This is determined by the band-edge discontinuity between heterolayers. The heterostructure integrated thermionic coolers (HIT) in Fig. 5 could operate in two modes. In the nonlinear regime, electron transport is dominated by the supply of electrons in the cathode layer. Since only hot electrons (with energy greater than

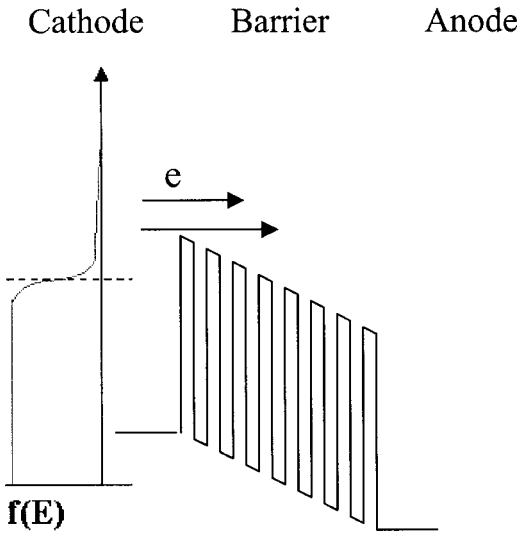

Fig. 5 Heterostructure thermionic emission for cooling at room temperatures.

E_f) are emitted above the barrier, electron-electron and electron-phonon interactions try to restore the quasi Fermi distributions in the cathode layer by absorbing heat from the lattice, thus cooling the layer. This heat is deposited on the anode side. Theoretical estimates by Shakouri and co-workers [7,32] show that there is an optimal barrier width of the order of a few electron energy relaxation lengths and an optimum barrier height of the order of k_BT, and that such heterostructure coolers can provide 20–30°C cooling with KW/cm^2 cooling density. Since the operating currents for the device is very high (10^5 A/cm^2), non-ideal effects such as the Joule heating at the metal-semiconductor contact resistance, and the reverse heat conduction have limited the experimental cooling results to <1°C. There is another regime of operation in which electron transport is dominated by the barrier structure. A superlattice is chosen so that hot electrons move easily in the materials, but the movement of cold electrons is more restricted. In this case, there will be also net cooling in the cathode layer and heating in the anode layer. Shakouri et al. [36] noted that a small barrier height on the order of k_BT does not give much improvement over bulk thermoelectric materials, and suggested tall barriers and high doping densities to achieve a large number of electrons moving in the material. To have a good HIT cooler, the barrier material should simply have an adequate electrical conductivity and a low thermal conductivity, making ternary and quaternary semiconductors good candidates.

On the experimental side, Shakouri and co-workers have fabricated thin-film thermoelectric coolers based on single heterojunction structures [37] and superlattice structures [38–42]. The SiGe/Si superlattice micro coolers can be monolithically integrated with Si-based microelectronic devices to achieve localized cooling and temperature control. Cooling by as much as 4.2 K at 25°C and 12 K at 200°C was measured on 3 μm thick, 60 $\times 60$ μm^2 devices. This corresponds to maximum cooling power densities approaching kW/cm^2. The micro cooler structure is based on cross-plane electrical transport. The main part of the cooler is a 3 μm strain-compensated SiGe/Si superlattice. It consists of 200 periods of (12 nm $Si_{0.75}Ge_{0.25}$/3 nm Si), doped with boron to about 6×10^{19} cm^{-3}. The $Si_{0.75}Ge_{0.25}$/Si superlattice has a valence band offset of about 0.16 eV, and hot holes going over this barrier can produce thermionic cooling. This superlattice was grown using molecular beam epitaxy (MBE). Its average lattice constant is that of $Si_{0.8}Ge_{0.2}$, and a buffer layer is required for it to be grown on a Si substrate. To reduce the material growth time in the MBE system, the buffer layer was grown on a p^+ (001) Si substrate by chemical vapor deposition (CVD) in the form of a graded SiGe structure. The boron doping in the buffer layer is 5×10^{19} cm^{-3}. Following the superlattice growth, a 0.3 μm $Si_{0.8}Ge_{0.2}$ cap layer was grown with a boron doping level of 2×10^{20} cm^{-3} to get a good ohmic contact to the device. Figure 6 shows a cross-section transmission electron microscopy (TEM) image of the MBE-grown SiGe/Si superlattice, and also a scanning electron micrograph of a micro cooler device. Figure 7 displays the measured cooling on 60×60 μm^2 superlattice cooler and a Si cooler at the heat sink temperature of 25°C. Figure 8 shows the temperature profile at a current of ~400 mA. One notices localized and uniform cooling on top of the micro refrig-

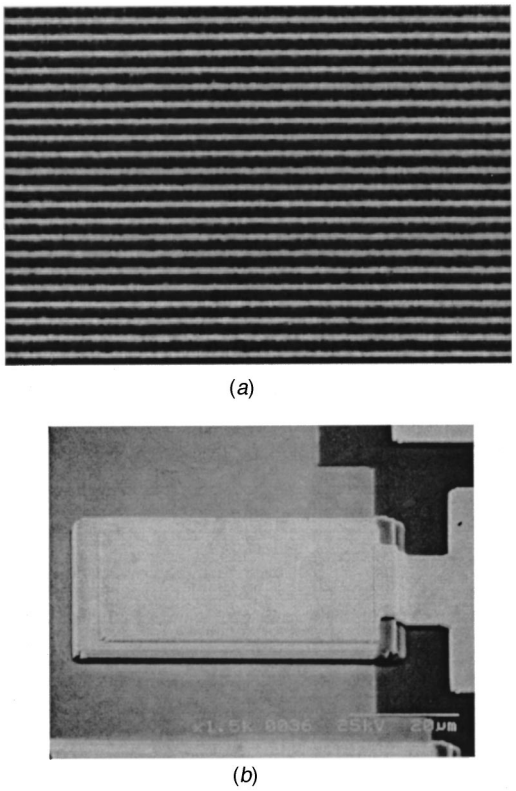

Fig. 6 (*a*) TEM image of the SiGe/Si superlattice (the dark parts are the 12 nm $Si_{0.75}Ge_{0.25}$ layers, the light parts are the 3 nm Si layers), and (*b*) a scanning electron micrograph of a fabricated micro refrigerator

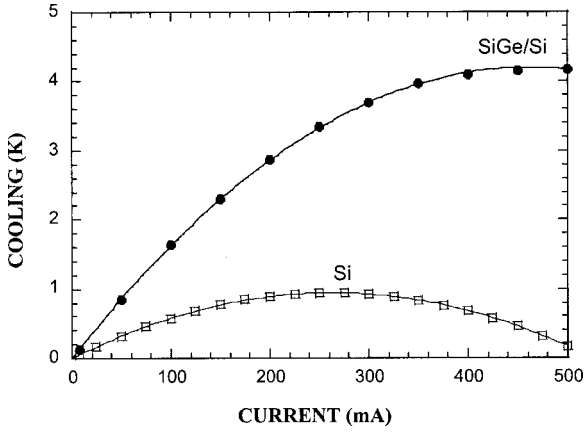

Fig. 7 Cooling measured on 60×60 μm^2 SiGe/Si superlattice coolers and on Si coolers at the heat sink temperature of 25°C

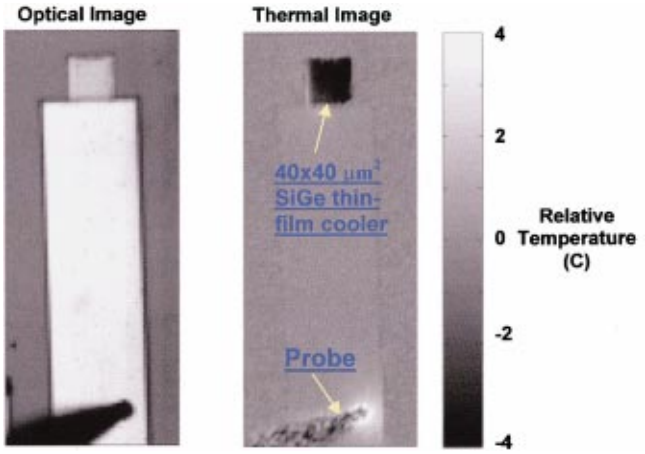

Fig. 8 Temperature distribution on top of a 40×40 micron square SiGe thin film cooler measured using thermoreflectance imaging. The applied current is ~400 mA.

erator as well as Joule heating near the probe on the side contact. With the use of a resistive heat load on top of the micro refrigerator, cooling power densities exceeding 500 W/cm^2 have been demonstrated [43].

Electron and phonon transport perpendicular to interfaces raise interesting heat transfer and energy conversion issues. One example is where heat is generated. Joule heating is often treated as a uniform volumetric heat generation. In heterostructures, the energy relaxation from electrons to phonons occurs over a distance comparable to the film thickness, and heat generation is no longer uniform. For single layer devices, this could benefit the device efficiency in principle [32,44]. Such non-uniform heat generation is a type of hot electron effect that has been studied in electronics [45], and has also be discussed quite extensively in the literature in the context of ultrafast laser-matter interactions [46]. Another example is the concurrent consideration of ballistic electron transport and ballistic phonon transport, coupled with nonequilibrium electron-phonon interaction. Zeng and Chen [47] started from the Boltzmann equations for electrons and phonons and obtained approximate solutions for the electron and phonon temperature distributions in heterostructures, as shown in Fig. 9. In this case, both electron and phonon temperatures show a discontinuity at the interface. The phonon temperature discontinuity is the familiar thermal boundary resistance phenomenon. Zeng and Chen concluded that in the nonlinear transport regime, it is the electron temperature discontinuity at the interface that determines the thermionic effect and the electron temperature gradient inside the film that determines the thermoelectric effect. Similar calculations by Vashaee and Shakouri [48] showed the importance of the electron-phonon coupling coefficient in the optimization of HIT coolers.

3.3 Phonon Thermal Conductivity Reduction Approach. Although phonons do not contribute directly to the energy conversion, the reduction of their contribution to the thermal conductivity is a central issue in thermoelectrics research. Several significant increases in the *ZT* of bulk materials were due to the introduction of thermal conductivity reduction strategies, such as the alloying [3] and phonon rattler concepts [49]. Size effects on phonon transport have long been established since the pioneering work by Casimir [50] at low-temperatures. Since the 1980s, the thermal conductivity reduction in thin films has drawn increasing attention. Naturally, the phonon thermal conductivity reduction in nanostructures has been considered as beneficial and even as a dominant approach to enhance *ZT* values.

One proposed approach is to use the thermal conductivity in the direction perpendicular to the superlattice film plane, or the cross-plane direction, while maintaining a low electronic band-edge offset, ideally no offset at all [9]. This would allow the electron transport across the interfaces without much scattering, while phonons would be scattered at the interfaces [51]. Some early experimental data [52,53] indicate that the thermal conductivity of superlattices could be significantly reduced, especially in the cross-plane direction. Tien and Chen [54] suggested the possibility of making super thermal insulators out of superlattices. Extensive experimental data on the thermal conductivity of various superlattices have been reported in recent years [51–65], mostly in the cross-plane direction. Following such a strategy, Venkatasubramanian's group has reported Bi_2Te_3/Se_2Te_3 superlattices with *ZT* values between 2-3 at room temperature. Although these results need to be confirmed due to the difficulty with the measurements, the reported data so far seem to support such claims and demonstrate that the thermal conductivity reduction is a very effective approach [9].

The mechanisms responsible for thermal conductivity reduction in low-dimensional structures thus have become a topic of considerable debate over the last few years. There have been many studies of the phonon spectrum and transport in superlattices since the original work by Narayanamurti et al. [66], but these works were focused on the phonon modes rather than on heat conduction. The first theoretical modeling predicted a small reduction of

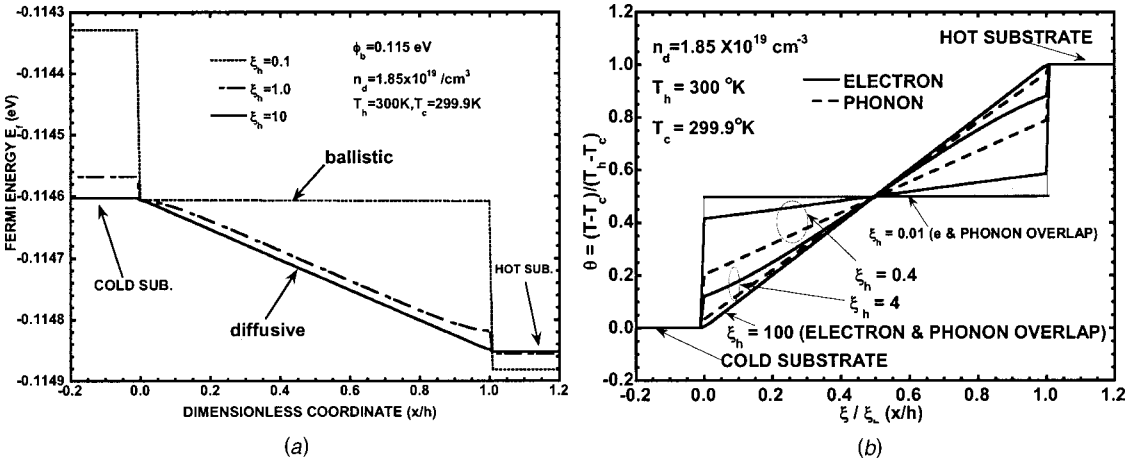

Fig. 9 Distribution of (*a*) Fermi level and (*b*) electron and phonon temperature inside double heterojunction structures. The dimensionless coordinate is normalized to the film thickness. ξ_h is the electron or phonon mean free path divided by the film thickness, n_d the carrier concentration and ϕ_b the barrier height.

the superlattice thermal conductivity [67] due to the formation of minigaps or stop bands. This predicted reduction, however, was too small compared to experiment results in recent years. Two major theoretical approaches were developed in the 1990s to explain the experimental results. One is based on solving the Boltzmann equation with the interfaces of the superlattice treated as boundary conditions [68–71]. The other is based on lattice dynamics calculation of the phonon spectrum and the corresponding change in the phonon group velocity [72–76]. More recently, there are also efforts to use molecular dynamics to simulate the thermal conductivity of superlattices directly [77,78].

Similar to the electron transport in superlattice structures, there could be several different regimes of phonon transport: the totally coherent regime, the totally incoherent regime, and the partially coherent regime. The lattice dynamics lies in the totally coherence regime. Such approaches are based on the harmonic force interaction assumption and thus do not consider anharmonic effects. A bulk relaxation time is often assumed. The main results out of the lattice dynamics models is that the phonon group velocity reduction caused by the spectrum change can lower the thermal conductivity by a factor of ~7–10 at room temperature for Si/Ge superlattices, and by a factor of 3 for GaAs/AlAs superlattices. Although it can be claimed that the predicted reduction in Si/Ge system is of the order of magnitude that is experimentally observed, the prediction clearly cannot explain the experimental results for GaAs/AlAs superlattices. The lattice dynamics model also showed that when the layers are 1–3 atomic-layers thick, there is a recovery of the thermal conductivity. The acoustic wave based model [79], which treats the superlattices as an inhomogeneous medium, shows a similar trend. It reveals that the thermal conductivity recovery is due to phonon tunneling and that the major source of the computed thermal conductivity reduction in the lattice dynamics model is the total internal reflection, which in the phonon spectrum representation, causes a group velocity reduction. For experimental results so far, the explanation of the thermal conductivity reduction based on the group velocity reduction has not been satisfactory even for the cross-plane direction. For the in-plane direction, the group velocity reduction alone leads to only a small reduction in thermal conductivity [76], and cannot explain the experimental data on GaAs/AlAs and Si/Ge superlattices [52,55,65]. There is a possibility that the change in the phonon spectrum creates a change in the relaxation time [80] but such a mechanism is unlikely to explain the experimental results for relatively thick-period superlattices since the density of states does not change in these structures [76].

Boltzmann equation-based models that treat phonons as particles transporting heat in inhomogeneous layers lie in the totally incoherent regime [68,71]. Theoretical calculations have been able to explain quantitatively the experimental data. The models are based on the solution of the Boltzmann equation using the relaxation time in the bulk materials for each layer. Phonon reflection and transmission at the interfaces are modeled based on past studies of the thermal boundary resistance. Compared to the lattice dynamics and acoustic waves models, the particle model allows the incorporation of diffuse interface scattering of phonons. In the models presented so far, the contribution of diffuse scattering has been left as a fitting parameter. In Fig. 10, we show the experimental in-plane and cross-plane thermal conductivity of a Si/Ge superlattice, together with simulation results based on the Boltzmann equation. One argument for the validity of the particle model is that thermal phonons have a short thermal wavelength, which is a measure of the coherence properties of broadband phonons inside the solid [68]. It is more likely, however, that the diffuse interface scattering, if it indeed happens as models suggested, destroys the coherence of monochromatic phonons and thus prevents the formation the superlattice phonon modes. The particle-based modeling can capture the effects of total internal reflection, which is partially responsible for the large group velocity reduction under the lattice dynamics models. Approximate

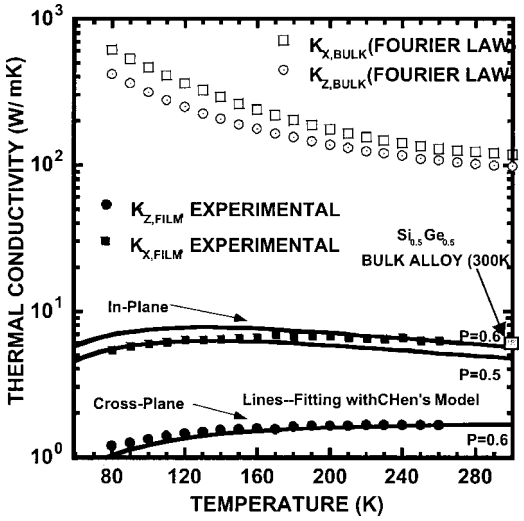

Fig. 10 Anisotropic thermal conductivity of the strained Si/Ge (20 Å /20 Å) superlattice: experimental data were fitted using Chen's models [68,71]. Also shown in the figure are comparisons of experimental data experimental data with predictions of Fourier theory based on bulk properties of each layer, and with compositionally equivalent alloy (300K) [65].

methods to incorporate phonon confinement or inelastic boundary scattering are also proposed. From the existing modeling, it can be concluded that for heat flow parallel to the interfaces, diffuse interface scattering is the key factor causing the thermal conductivity reduction. For the case of heat conduction perpendicular to the interfaces, phonon reflection, confinement, as well as diffuse scattering can greatly reduce the heat transfer and thermal conductivity. The larger the reflection coefficient, the larger is the thermal conductivity reduction in the cross-plane direction.

A key unsolved issue is what are the actual mechanisms of phonon scattering at the interfaces, particularly what causes the diffuse phonon scattering. Phonon scattering has been studied quite extensively in the past in the context of thermal boundary resistance. Superlattice structures that are grown by epitaxy techniques usually have better interface morphology than the other types of interfaces studied previously. Even for the best material system such as GaAs/AlAs, however, the interfaces are not perfect. There is interface mixing and there are also regions with monolayer thickness variation. These are naturally considered as potential sources of diffuse interface scattering for which a simplified model was developed by Ziman [82]. Another possibility is the anharmonic force between the atoms in two adjacent layers. Boltzmann equation-based modeling assumes a constant parameter p to represent the fraction of phonons specularly scattered. Ju and Goodson [81] used an approximate frequency-dependent expression for p given by Ziman [82] in the interpretation of the thermal conductivity of single layer silicon films. Chen [71] also argued that inelastic scattering occurring at interfaces can provide a path for the escape of confined phonons. A promising approach to resolve this issue is molecular dynamics simulation [77,78]. In addition to the interface scattering mechanisms, there are also several other unanswered questions. For example, experimental data of Venkatasubrmanian seems to indicate a butterfly-shaped thermal conductivity curve as a function of thickness [9,83]. Quantitative modeling of the stress and dislocation effects also needs to be further refined.

Since the lattice dynamics and the particle models present the totally coherent and totally incoherent regimes, a theoretical approach that can include both effects should be sought. Simkin and Mahan [84] proposed a new lattice dynamics model by the introduction of an imaginary wavevector that is related to the mean free path. This approach leads to the prediction of a minimum in

the thermal conductivity value as a function of the superlattice period thickness. For thicknesses larger than the minimum, the thermal conductivity increases with thickness and eventually approaches the bulk values. For thicknesses thinner than the minimum, the thermal conductivity recovers to a higher value. However, it should be pointed out that the imaginary wavevector represents an absorption process, not exactly a scattering process, as is clear in the meaning of the extinction coefficient of the optical constants. It will be interesting to see whether such an approach can explain the experimental observed trends of thermal conductivity reduction along the in-plane direction.

Aside from superlattices and thin films, other low-dimensional structures such as quantum wires and quantum dots are also being considered for thermoelectric applications. There are a few experimental and theoretical studies on the thermal conductivity of quantum dot arrays and nanostructured porous medium [85,86]. Theoretically, one can expect a larger thermal conductivity reduction in quantum wires compared to thin films [87,88]. The measurements of the thermal conductivity in quantum wires have been challenging. Recent measurements on the thermal conductivity of carbon nanotubes provide possible approach for measurements on nanowires for thermoelectric applications [89]. Nanowires for thermoelectric applications, however, usually have a low thermal conductivity, which may need different characterization techniques.

4 Characterization

The characterization of thermoelectric properties has turned out to be the most challenging issue for the development of nanostructure-based thermoelectric materials. First, the thermal conductivity measurements for even bulk materials are not easy. For thin films, these measurements become even more difficult. Even the normally easier measurements in bulk materials, such as for the electrical conductivity and the Seebeck coefficient, can be complicated due to the small thickness of the film and the contributions from the substrate.

It is generally recognized that the thermal conductivity is the most difficult parameter to measure. Fortunately, thin film thermal conductivity measurements have drawn considerable attention over the past two decades and different methods have been developed. One popular method to measure the thermal conductivity of thin films is the 3ω method [90,91]. For thermoelectric thin films such as superlattices, there are several complications. For example, thermoelectric films are semiconductors and thus an insulating film is required between the heater and the film. The superlattice thermal conductivity is highly anisotropic. The 3ω method is typically applied to measure the cross-plane thermal conductivity by ensuring that the heater width is much larger than the film thickness. Often, an additional buffer layer exists between the film and the substrate. For Si/Ge, the buffer is graded and thus has a continuously varying thermal conductivity profile. In applying the 3ω method, there is also the contrast factor that must be considered between the film and the substrate. When the film and the substrate have close properties, more complicated modeling is needed. By careful modeling and experimental design, the 3ω method can be applied to a wide range of thin films for measuring the thermal conductivity in both in-plane and cross-plane directions [92]. Other methods such as ac calorimetry, photothermal and pump-and-probe methods have also been used to measure the thermal diffusivity of superlattices. References [10], [93–96] provide detailed reviews of existing methods. By assuming that the specific heat does not change much, which is usually a valid assumption, the thermal conductivity of the structures can be calculated from the measured diffusivity.

Although the measurement of the electrical conductivity and Seebeck coefficient is considered relatively straight-forward for bulk materials, it has turned out to be much more complicated for thin films. For transport along the thin film plane, the complications arise from the fact that most thin films are deposited on semiconductor substrates and the thermoelectric effect of the substrates can overwhelm that of the films. To circumvent these difficulties, several approaches have been taken, such as removing the substrate or growing the film on insulating layers. For example, Si/Ge superlattices are grown on silicon-on-insulator structures. Even with these precautions, there are still complications such as the existence of the buffer. Thus, differential measurements are sometimes used to subtract the influence of the buffer layer. For transport in the cross-plane direction, measurements of the electrical conductivity and Seebeck effect become much more difficult because the films are usually very thin. The recently reported ZT values between 2–3 for Bi_2Te_3/Se_2Te_3 superlattices were obtained using the transient Harman method [9]. Although the method is well established for bulk materials, the application to thin film structures requires careful consideration of various heat losses and heat generation through the leads. This is a topic that has yet to be fully addressed. In addition, the transient Harman method gives ZT rather than individual thermoelectric properties such as the Seebeck coefficient. A comparative method was recently developed to measure the Seebeck coefficient in the cross-plane direction of the superlattices [97].

5 Micro Devices and Potential Applications

Although thermoelectric coolers and power generators are intrinsically smaller than conventional coolers and power generators, on the order of a few millimeters to centimeters, there are major efforts to develop microscale thermoelectric devices for several reasons. (1) Monolithic integration is desirable for the cooling and temperature stabilization of electronic and phononic devices. (2) Heat flux that can be handled by coolers increases as the device thickness decreases. Of course, smaller device sizes are attractive for their weight and volume. Several types of thermoelectric microdevices are being developed. Figures 7 and 8 show device performance based on Si/Ge superlattices with transport in the cross-plane direction. Another approach is to use electrodeposited films [98] to make microdevices. Efforts exist in using micromachining of bulk thermoelectric materials to make microdevices [99,100]. Devices based on transport along the film plane are also being pursued, for applications in detectors and power sources [101,102].

As the device length becomes smaller, several degradation factors become important and must be addressed. These include (1) the electrical contact resistance, (2) thermal contact resistance, (3) heat sink thermal resistance in both the hot and the cold sides, and (4) additional heat leaks caused by contacts. For transport perpendicular to the film plane, the most important issues are the electrical contact resistance, the thermal boundary resistance and the spreading resistance in the hot and the cold regions. For transport along the film plane, heat leakage through the support layers normally requires the removal of the substrate. Even without a substrate, the heat leakage through the supporting membrane and the buffer layers can significantly degrade the device performance, particularly when the thermoelectric film is very thin.

5.1 Applications. Thermoelectric microdevices have some immediate applications. If the reported ZT is further confirmed and enhanced, the applications will undoubtly expand into many areas. Here, we will discuss a number of potential applications: (1) temperature stabilization, (2) high cooling density spot cooling, and (3) micropower generation.

Temperature stabilization is very important for optoelectronic devices such as laser sources, switching/routing elements, and detectors. They require careful control over their operating temperature. This is especially true in current high speed and wavelength division multiplexed (WDM) optical communication networks. Long haul optical transmission systems operating around 1.55 μm wavelength typically use erbium-doped fiber amplifiers (EDFA's), and are restricted in the wavelengths they can use due to the finite bandwidth of these amplifiers. As more channels are packed into this wavelength window, the spacing between adjacent channels

becomes smaller and wavelength drift becomes very important. Temperature variations are the primary cause for the wavelength drift, and they also affect the threshold current and output power in laser sources. Most stable sources such as distributed feedback (DFB) lasers and vertical cavity surface emitting lasers (VCSEL's) can generate large heat power densities on the order of kW/cm^2 over areas as small as 100 μm^2 [103,104]. The output power for a typical DFB laser changes by approximately 0.4 dB/°C. Typical temperature-dependent wavelength shifts for these laser sources are on the order of 0.1 nm/°C [105]. Therefore, a temperature change of only a few degrees in a WDM system with a channel spacing of 0.2–0.4 nm would be enough to switch data from one channel to the adjacent one, and even less of a temperature change could dramatically increase the crosstalk between two channels. Temperature stabilization or refrigeration is commonly performed with conventional thermoelectric (TE) coolers. However since their integration with optoelectronic devices is difficult [103,106], component cost is greatly increased because of packaging. The reliability and lifetime of packaged modules are also usually limited by their TE coolers [107]. Microdevices monolithically integrated with the functioning optoelectronic devices have advantages over separate devices in terms of their response time, size, and costs.

Many electronic and optoelectronic devices dissipate high heat flux. Conventional thermoelectric devices cannot handle large heat flux. With reduced leg length, the cooling heat flux of thermoelectric devices increases, thus providing the opportunity to handle high heat flux devices. It should be remembered, however, that more heat flux must be rejected at the hot side and must be removed using conventional heat transfer technologies such as heat pipes and high thermal conductivity heat spreaders. The active cooling method is beneficial only when the device needs to be operated below ambient temperatures or for temperature stabilization. Examples are infrared detectors and quantum cascade lasers. The speed of many electronic devices increases with reduced temperature and thus it is possible to use thermoelectric coolers to gain increased speed. Instead of cooling the whole chip, thermoelectric microcoolers can potentially be applied to handle local hot spots in semiconductor chips [108]. Regions with sizes ranging from 10's to 100's of micron in diameter have a temperature 10–30°C higher than the average chip temperature. This causes clock delays and failures in digital circuits. In addition, chip reliability due to electromigration is a thermally activated process, so the mean-free time between failures decreases exponentially as the temperature rises.

Thermoelectric devices have traditionally been used as radiation detectors such as thermopiles and can be used as power sources. With the rapid developments in MEMS, microscale power supply has been in increasing demands. Thermoelectric micro-generators can be coupled with environmental heat sources to drive sensors and microdevices for automanous operation of these devices. The body temperature powered wristwatch is a recent example [109].

6 Concluding Remarks

In this paper, we discuss recent progress in nanostructure-based solid-state energy conversion. Energy transport for both electrons and phonons can differ significantly from that in bulk materials. The nanoscale size effects can be used to improve the energy conversion efficiency. Recent studies have led to quite a large increase in *ZT* values and significant new insights into thermoelectric transport in nanostructures. There is, however, much left to be done in new materials syntheses, characterization, physical understanding, and device fabrication. This is a research area that the heat transfer community can both benefit from and contribute to. Meanwhile, we would like to emphasize that thermoelectric materials research is a multidisciplinary endeavor and requires close collaboration among researchers to address issues in materials, theory, characterization, and devices. Among these issues, heat transfer plays a significant role.

Acknowledgments

G. C. would like to acknowledge supports from NSF, DoD/ONR MURI on Thermoelectrics and DARPA HERETIC project for the work reported here. He would like to thank Professors M. S. Dresselhaus, K. L. Wang, T. Sands, and R. Gronsky, and their students for their contributions to the discussed work. A. S. acknowledges support from the Packard Foundation, NSF and DARPA HERETIC project. He would like to thank Professors J. Bowers, A. Majumdar, V. Narayanamurti, their students, and Dr. Ed. Croke for their contributions to the work presented here.

Nomenclature

C = spectral volumetric specific heat, $J\,m^{-3}Hz^{-1}K^{-1}$
D = density of states per unit volume, $J^{-1}m^{-3}$
E = energy relative to band edge, J
E_f = Fermi level relative to band edge, J
f = electron distribution function
f_{eq} = equilibrium distribution function
$\mathbf{J}$ = current density, $A\,m^{-2}$
$\mathbf{J}_q$ = heat flux, $W\,m^{-2}$
k = thermal conductivity, $W\,m^{-1}K^{-1}$
$\mathbf{k}$ = wavevector
k_B = Boltzmann constant, $J\,K^{-1}$
L_n = transport coefficients defined by Eq. (8)
q = charge per carrier, C
$\mathbf{r}$ = coordinate
S = Seebeck coefficient, $V\,K^{-1}$
t = time, s
T = temperature, K
v = velocity, $m\,s^{-1}$
Z = figure of merit, K^{-1}
$\boldsymbol{\varepsilon}$ = electrical field, V/m
Φ = electrochemical potential, J
σ = electrical conductivity $\Omega^{-1}m^{-1}$, or differential conductivity, $\Omega^{-1}m^{-1}J^{-1}$
τ = relaxation time, s
ω = angular frequency, rad . Hz

References

[1] Goldsmid, H. J., 1964, *Thermoelectric Refrigeration*, Plenum Press, New York.
[2] Rowe, D. M., ed., 1995, *Handbook of Thermoelectrics*, CRC Press, Boca Raton.
[3] Ioffe, A. F., 1957, *Semiconductor Thermoelements and Thermoelectric Cooling*, Infosearch Limited, London.
[4] Tritt, T. M., ed., 2001, "Recent Trend in Thermoelectric Materials Research," in *Semiconductors and Semimetals*, Vol. 69-Vol. 71, Academic Press, San Diego.
[5] Hicks, L. D., and Dresselhaus, M. S., 1993, "Effect of Quantum-Well Structures on the Thermoelectric Figure of Merit," Phys. Rev. B, **47**, pp. 12727–12731.
[6] Dresselhaus, M. S., Lin, Y. M., Cronin, S. B., Rabin, O., Black, M. R., Dresselhaus, G., and Koga, T., 2001, "Quantum Wells and Quantum Wires for Potential Thermoelectric Applications," in Semicond. Semimetals, **71**, pp. 1–121.
[7] Shakouri, A., and Bowers, J. E., 1997, "Heterostructure Integrated Thermionic Coolers," Appl. Phys. Lett., **71**, pp. 1234–1236.
[8] Mahan, G. D., 2001, "Thermionic Refrigeration," Semicond. Semimetals, **71**, pp. 157–174.
[9] Venkatasubramanian, R., 2001, "Phonon Blocking Electron Transmitting Superlattice Structures as Advanced Thin Film Thermoelectric Materials," Semicond. Semimetals, **71**, pp. 175–201.
[10] Chen, G., 2001, "Phonon Transport in Low-Dimensional Structures," Semicond. Semimetals, **71**, pp. 203–259.
[11] Harman, T. C., Taylor, P. J., Spears, D. L., and Walsh, M. P., 2000, "Thermoelectric Quantum-Dot Superlattices with High ZT," J. Electron. Mater., **29**, pp. L1–L4.
[12] Dubios, L., 1999, "An Introduction to the DARPA Program in Advanced Thermoelectric Materials and Devices," *Proc. Int. Conf. Thermoelectrics*, ICT'99, pp. 1–4.
[13] Aschroft, N. W., and Mermin, N. D., 1976, *Solid State Physics*, Saunders College Publishing, Fort Worth.

[14] Mahan, G. D., and Sofo, J. O., 1996, ''The Best Thermoelectric,'' Proc. Natl. Acad. Sci. U.S.A., **93**, pp. 7436–7439.
[15] Sun, X., Cronin, S. B., Liu, J. L., Wang, K. L., Koga, T., Dresselhaus, M. S., and Chen, G., 1999, ''Experimental Study of the Effect of the Quantum Well Structures on the Thermoelectric Figure of Merit in Si/SixGel-x System,'' *Proceedings of Int. Conf. Thermoelectrics*, ICT'99, pp. 652–655.
[16] Broido, D. A., and Reinecke, T. L., 1995, ''Effect of Superlattice Structure on the Thermoelectric Figure of Merit,'' Phys. Rev. B, **51**, pp. 13797–13800.
[17] Sofo, J. O., and Mahan, G. D., 1994, ''Thermoelectric Figure of Merit of Superlattices,'' Appl. Phys. Lett., **65**, pp. 2690–2692.
[18] Koga, T., Sun, X., Cronin, S. B., and Dresselhaus, M. S., 1998, ''Carrier Pocket Engineering to Design Superior Thermoelectric Materials Using GaAs/AlAs Superlattices,'' Appl. Phys. Lett., **73**, pp. 2950–2952.
[19] Koga, T., Cronin, S. B., Dresselhaus, M. S., Liu, J. L., and Wang, K. L., 2000, ''Experimental Proof-of-Principle Investigation of Enhanced $Z_{3D}T$ in (001) Oriented Si/Ge Superlattices,'' Appl. Phys. Lett., **77**, pp. 1490–1492.
[20] Chen, G., 1997, ''Size and Interface Effects on Thermal Conductivity of Superlattices and Periodic Thin-Film Structures,'' ASME J. Heat Transfer , **119**, pp. 220–229 (see also Proc. 1996 Nat. Heat Transf. Conf., ASME HTD-Vol. 323, **121**, 1996).
[21] Hicks, L. D., Harman, T. C., and Dresselhaus, M. S., 1996, ''Experimental Study of the Effect of Quantum-Well Structures on the Thermoelectric Figure of Merit,'' Phys. Rev. B, **53**, pp. 10493–10496.
[22] Harman, T. C., Taylor, P. J., Spears, D. L., and Walsh, M. P., 2000, ''Thermoelectric Quantum-Dot Superlattices With High ZT,'' J. Electron. Mater., **29**, pp. L1–L4.
[23] Whitlow, L. W., and Hirano, T., 1995, ''Superlattice Application to Thermoelectricity,'' J. Appl. Phys., **78**, pp. 5460–5466.
[24] Radtke, R. J., Ehrenreich, H., and Grein, C. H., 1999, ''Multilayer Thermoelectric Refrigeration in $Hg_{1-x}Cd_xTe$ Superlattices,'' J. Appl. Phys., **86**, pp. 3195–3198.
[25] Kumar, R., Borca-Tasciuc, D., Zeng, T., and Chen, G., 2000, ''Thermal Conductivity of Nanochanneled Alumina,'' *Proc. Int. Mech. Eng. Congress and Exhibition* (IMECE2000), ASME HTD-Vol. 366-2, pp. 393–398.
[26] Zhang, Z. B., Gekhtman, D., Dresselhaus, M. S., and Ying, J. Y., 1999, ''Processing and Characterization of Single-Crystalline Ultrafine Bismuth Nanowires,'' Chem. Mater., **11**, pp. 1659–1665.
[27] Heremans, J., Thrush, C. M., Lin, Y. M., Cronin, S., and Dresselhaus, M. S., 2000, ''Bismuth Nanowire Arrays: Synthesis and Galvanomagnetic Properties,'' Phys. Rev. B, **61**, pp. 2921–2930.
[28] Behnke, J. F., Prieto, A. L., Stacy, A. M., and Sands, T., 1999, ''Electrodeposition of $CoSb_3$ Nanowires,'' ICT'99 pp. 451–453.
[29] Hatsopoulos, G. N., and Kaye, J., 1958, ''Measured Thermal Efficiencies of a Diode Configuration of a Thermo Electron Engine,'' J. Appl. Phys., **29**, pp. 1124–1125.
[30] Mahan, G. D., 1994, ''Thermionic Refrigeration,'' J. Appl. Phys., **76**, pp. 4362–4366.
[31] Mahan, G. D., and Woods, L. M., 1998, ''Multilayer Thermionic Refrigeration,'' Phys. Rev. Lett., **80**, pp. 4016–4019.
[32] Shakouri, A., Lee, E. Y., Smith, D. L., Narayanamurti, V., and Bowers, J. E., 1998, ''Thermoelectric Effects in Submicron Heterostructure Barriers,'' Microscale Thermophys. Eng., **2**, pp. 37–42.
[33] Moyzhes, B., and Nemchinsky, V., 1998, ''Thermoelectric Figure of Merit of Metal-Semiconductor Barrier Structure based on Energy Relaxation Length,'' Appl. Phys. Lett., **73**, pp. 1895–1897.
[34] Miskovsky, N. M., and Cutler, P. H., 1999, ''Microelectronic Cooling Using the Nottingham Effect and Internal Field Emission in a Diamond (Wide-Band Gap Material) Thin-Film Device,'' Appl. Phys. Lett., **75**, pp. 2147–2149.
[35] Korotkov, A. N., and Likharev, K. K., 1999, ''Possible Cooling by Resonant Fowler-Nordheim Emission,'' Appl. Phys. Lett., **75**, pp. 2491–2493.
[36] Shakouri, A., Labounty, C., Abraham, P., Piprek, J., and Bowers, J. E., 1998, ''Enhanced Thermionic Emission Cooling in High Barrier Superlattice Heterostructures,'' Mater. Res. Soc. Symp. Proc., **545**, pp. 449–458.
[37] Shakouri, A., LaBounty, C., Piprek, J., Abraham, P., and Bowers, J. E., 1999, ''Thermionic Emission Cooling in Single Barrier Heterostructures,'' Appl. Phys. Lett., **74**, pp. 88–89.
[38] Zeng, G. H., Shakouri, A., La Bounty, C., Robinson, G., Croke, E., Abraham, P., Fan, X. F., Reese, H., and Bowers, J. E., 1999, ''SiGe Micro-Cooler,'' Electron. Lett., **35**, pp. 2146–2147.
[39] Fan, X. F., Zeng, G. H., LaBounty, C., Bowers, J. E., Croke, E., Ahn, C. C., Huxtable, S., Majumdar, A., and Shakouri, A., 2001, ''SiGeC/Si Superlattice Microcoolers,'' Appl. Phys. Lett., **78**, pp. 1580–1582.
[40] Fan, X. F., Zeng, G., Croke, E., LaBounty, C., Ahn, C. C., Vashaee, D., Shakouri, A., and Bowers, J. E., 2001, ''High Cooling Power Density SiGe/Si Micro-Coolers,'' Electron. Lett., **37**, pp. 126–127.
[41] LaBounty, C., Shakouri, A., Abraham, P., and Bowers, J. E., 2000, ''Monolithic Integration of Thin-Film Coolers with Optoelectronic Devices,'' Opt. Eng., **39**, pp. 2847–2852.
[42] LaBounty, C., Shakouri, A., and Bowers, J. E., 2001, ''Design and Characterization of Thin Film Microcoolers,'' J. Appl. Phys., **89**, pp. 4059–4064.
[43] Zeng, G., Fan, X., LaBounty, C., Bowers, J. E., Croke, E., and Shakouri, A., ''Direct Measurements of Cooling Power Density for SiGe/Si Superlattice Microcoolers,'' submitted for publication.
[44] Zeng, T. F., and Chen, G., 2000, ''Energy Conversion in Heterostructures for Thermionic Cooling,'' Microscale Thermophys. Eng., **4**, pp. 39–50.
[45] Reggiani, L., ed., 1985, *Hot-Electron Transport in Semiconductors*, Springer-Verlag.
[46] Qiu, T. Q., and Tien, C. L., 1993, ''Heat Transfer Mechanisms During Short-Pulse Laser Heating of Metals,'' ASME J. Heat Transfer , **115**, pp. 835–841.
[47] Zeng, T. F., and Chen, G., 2000, ''Nonequilibrium Nonequilibrium Electron and Phonon Transport in Heterostructures for Energy Conversion,'' *Proceedings of Int. Mech. Eng. Congress and Exhibition* (IMECE2000), ASME HTD-Vol. 366-2, pp. 361–372.
[48] Vashaee, D., and Shakouri, A., 2002, unpublished.
[49] Nolas, G. S., Slack, G. A., Morelli, D. T., Tritt, T. M., and Ehrlich, A. C., 1996, ''The Effect of Rare-Earth Filling on the Lattice Thermal Conductivity of Skutterudites,'' J. Appl. Phys., **79**, pp. 4002–4008.
[50] Casimir, H. B. G., 1938, ''Note on the Conduction of Heat in Crystals,'' Physica, **5**, pp. 495–500.
[51] Venkatasubramanian, R., 1996, ''Thin-Film Superlattice and Quantum-Well Structures—A New Approach to High-Performance Thermoelectric Materials,'' Nav. Res. Rev., **58**, pp. 44–54.
[52] Yao, T., 1987, ''Thermal Properties of AlAs/GaAs Superlattices,'' Appl. Phys. Lett., **51**, pp. 1798–1800.
[53] Chen, G., Tien, C. L., Wu, X., and Smith, J. S., 1994, ''Measurement of Thermal Diffusivity of GaAs/AlGaAs Thin-Film Structures,'' ASME J. Heat Transfer , **116**, pp. 325–331.
[54] Tien, C. L., and Chen, G., 1994, ''Challenges in Microscale Conductive and Radiative Heat Transfer,'' ASME J. Heat Transfer , **116**, pp. 799–807.
[55] Yu, X. Y., Chen, G., Verma, A., and Smith, J. S., 1995, ''Temperature Dependence of Thermophysical Properties of GaAs/AlAs Periodic Structure,'' Appl. Phys. Lett. **67**, pp. 3554–3556, p. 1303.
[56] Capsinski, W. S., and Maris, H. J., 1996, ''Thermal Conductivity of GaAs/AlAs Superlattices,'' Physica B, **220**, pp. 699–701.
[57] Lee, S. M., Cahill, D. G., and Venkatasubramanian, R., 1997, ''Thermal Conductivity of Si-Ge Superlattices,'' Appl. Phys. Lett., **70**, pp. 2957–2959.
[58] Yamasaki, I., Yamanaka, R., Mikami, M., Sonobe, H., Mori, Y., and Sasaki, T., 1998, ''Thermoelectric Properties of Bi_2Te_3 /Sb_2Te_3 Superlattice Structures,'' *Proc. Int. Conf. Thermoelectrics*, ICT'98, pp. 210–213.
[59] Capinski, W. S., Maris, H. J., Ruf, T., Cardona, M., Ploog, K., and Katzer, D. S., 1999, ''Thermal-Conductivity Measurements of GaAs/AlAs Superlattices Using a Picosecond Optical Pump-and-Probe Technique,'' Phys. Rev. B, **59**, pp. 8105–8113.
[60] Borca-Tasciuc, T., Liu, W. L., Zeng, T., Song, D. W., Moore, C. D., Chen, G., Wang, K. L., Goorsky, M. S., Radetic, T., Gronsky, R., Koga, T., and Dresselhaus, M. S., 2000, ''Thermal Conductivity of Symmetrically Strained Si/Ge Superlattices,'' Superlattices Microstruct., **28**, pp. 119–206.
[61] Song, D. W., Liu, W. L., Zeng, T., Borca-Tasciuc, T., Chen, G., Caylor, C., and Sands, T. D., 2000, ''Thermal Conductivity of Skutterudite Thin Films and Superlattices,'' Appl. Phys. Lett., **77**, pp. 3854–3856.
[62] Venkatasubramanian, R., 2000, ''Lattice Thermal Conductivity Reduction and Phonon Localizationlike Behavior in Superlattice Structures,'' Phys. Rev. B, **61**, pp. 3091–3097.
[63] Huxtable, S. T., Shakouri, A., LaBounty, C., Fan, X., Abraham, P., Chiu, Y. J., Chiu, Y. J., and Majumdar, A., 2000, ''Thermal Conductivity of Indium Phosphide-Based Superlattices,'' Microscale Thermophys. Eng., **4**, pp. 197–203.
[64] Borca-Tasciuc, T., Achimov, D., Liu, W. L., Chen, G., Ren, H.-W., Lin, C.-H., and Pei, S. S., 2001, ''Thermal Conductivity of InAs/AlSb Superlattices,'' Microscale Thermophys. Eng., **5**, pp. 225–231.
[65] Liu, W. L., Borca-Tasciuc, T., Chen, G., Liu, J. L., and Wang, K. L., 2001, ''Anisotropy Thermal Conductivity of Ge-Quantum Dot and Symmetrically Strained Si/Ge Superlattice,'' J. Nanosci. Nanotech., **1**, pp. 39–42.
[66] Narayanamurti, V., Stormer, J. L., Chin, M. A., Gossard, A. C., and Wiegmann, W., 1979, ''Selective Transmission of High-Frequency Phonons by a Superlattice: the Dielectric Phonon Filter,'' Phys. Rev. Lett., **43**, pp. 2012–2015.
[67] Ren, S. Y., and Dow, J., 1982, ''Thermal Conductivity of Superlattices,'' Phys. Rev. B, **25**, pp. 3750–3755.
[68] Chen, G., 1997, ''Size and Interface Effects on Thermal Conductivity of Superlattices and Periodic Thin-Film Structures,'' ASME J. Heat Transfer, **119**, pp. 220–229.
[69] Hyldgaard, P., and Mahan, G. D., 1996, ''Phonon Knudson Flow in Superlattices,'' Therm. Conduct., **23**, p. 172–181.
[70] Chen, G., and Neagu, M., 1997, ''Thermal Conductivity and Heat Transfer in Superlattices,'' Appl. Phys. Lett., **71**, pp. 2761–2763.
[71] Chen, G., 1998, ''Thermal Conductivity and Ballistic Phonon Transport in Cross-Plane Direction of Superlattices,'' Phys. Rev. B, **57**, pp. 14958–14973.
[72] Hyldgaard, P., and Mahan, G. D., 1997, ''Phonon Superlattice Transport,'' Phys. Rev. B, **56**, pp. 10754–10757.
[73] Tamura, S., Tanaka, Y., and Maris, H. J., 1999, ''Phonon Group Velocity and Thermal Conduction in Superlattices,'' Phys. Rev. B, **60**, pp. 2627–2630.
[74] Bies, W. E., Radtke, R. J., and Ehrenreich, H., 2000, ''Phonon Dispersion Effects and the Thermal Conductivity Reduction in GaAs/AlAs Superlattices,'' J. Appl. Phys., **88**, pp. 1498–1503.
[75] Kiselev, A. A., Kim, K. W., and Stroscio, M. A., 2000, ''Thermal Conductivity of Si/Ge Superlattices: A Realistic Model with a Diatomic Unit Cell,'' Phys. Rev. B, **62**, pp. 6896–6899.
[76] Yang, B., and Chen, G., 2001, ''Anisotropy of Heat Conduction in Superlattices,'' Microscale Thermophys. Eng., **5**, pp. 107–116.
[77] Volz, S. G., Saulnier, J. B., Chen, G., and Beauchamp, P., 2000, ''Computation of Thermal Conductivity of Si/Ge Superlattices by Molecular Dynamics Techniques,'' Microelectronics J., **31**, pp. 815–819.
[78] Liang, X. G., and Shi, B., 2000, ''Two-Dimensional Molecular Dynamics

Simulation of the Thermal Conductance of Superlattices with Lennard-Jones Potential,'' Mater. Sci. Eng., **292**, pp. 198–202.
[79] Chen, G., 1999, ''Phonon Wave Heat Conduction in Thin Films and Superlattices,'' ASME J. Heat Transfer , **121**, pp. 945–953.
[80] Balandin, A., and Wang, K. L., 1998, ''Effect of Phonon Confinement on the Thermoelectric Figure of Merit of Quantum Wells,'' J. Appl. Phys., **84**, pp. 6149–6153.
[81] Ju, Y. S., and Goodson, K. E., 1999, ''Phonon Scattering in Silicon Films with Thickness of Order 100 nm,'' Appl. Phys. Lett., **74**, pp. 3005–3007.
[82] Ziman, J. M., 1960, *Electrons and Phonons*, Clarendon Press, Oxford.
[83] Venkatasubramian, R., Siivola, E., and Colpitts, T. S., 1998, ''In-Plane Thermoelectric Properties of Freestanding Si/Ge Superlattice Structures,'' *Proc. Int. Conf. Thermoelectrics*, ICT'98, pp. 191–197.
[84] Simkin, M. V., and Mahan, G. D., 2000, ''Minimum Thermal Conductivity of Superlattices,'' Phys. Rev. Lett., **84**, pp. 927–930.
[85] Arutyunyan, L. I., Bogomolov, V. N., Kartenko, N. F., Kurdyukov, D. A., Popov, V. V., Prokof'ev, A. V., Smirnov, I. A., and Sharenkova, N. V., 1997, ''Thermal Conductivity of a New Type of Regular-Structure Nanocomposites: PbSe in Opal Pores,'' Phys. Solid State, **39**, pp. 510–514.
[86] Song, D. W., Shen, W.-N., Zeng, T., Liu, W. L., Chen, G., Dunn, B., Moore, C. D., Goorsky, M. S., Radetic, R., and Gronsky, R., 1999, ''Thermal Conductivity of Nano-Porous Bismuth Thin Films for Thermoelectric Applications,'' ASME HTD-Vol. 364-1, pp. 339–344.
[87] Volz, S. G., and Chen, G., 1999, ''Molecular Dynamics Simulation of Thermal Conductivity of Si Nanowires,'' Appl. Phys. Lett., **75**, pp. 2056–2058.
[88] Walkauskas, S. G., Broido, D. A., Kempa, K., and Reinecke, T. L., 1999, ''Lattice Thermal Conductivity of Wires,'' J. Appl. Phys., **85**, pp. 2579–2582.
[89] Kim, P., Shi, L., Majumadar, A., and McEuen, P. L., 2001, ''Thermal Transport Measurements on Individual Multi-walled Nanotubes,'' Phys. Rev. Lett., **87**, p. 215502.
[90] Cahill, D. G., 1990, ''Thermal Conductivity Measurement from 30-K to 750-K—The 3-Omega Method,'' Rev. Sci. Instrum., **61**, pp. 802–808.
[91] Lee, S. M., and Cahill, D. G., 1997, ''Heat Transport in Thin Dielectric Films,'' J. Appl. Phys., **81**, pp. 2590–2595.
[92] Borca-Tasciuc, T., Kumar, R., and Chen, G., 2001, ''Data Reduction in 3ω Method for Thin Film Thermal Conductivity Measurements,'' Rev. Sci. Instrum., **72**, pp. 2139–2147.
[93] Cahill, D. G., Fischer, H. E., Klitsner, T., Swartz, E. T., and Pohl, R. O., 1989, ''Thermal Conductivity of Thin Films: Measurement and Understanding,'' J. Vac. Sci. Technol. A, **A7**, pp. 1259–1266.
[94] Hatta, I., 1990, ''Thermal Diffusivity Measurement of Thin Films and Multilayered Composites,'' Int. J. Thermophys., **11**, pp. 293–303.
[95] Volklein, F., and Starz, T., 1997, ''Thermal Conductivity of Thin Films—Experimental Methods and Theoretical Interpretation,'' *Proc. Int. Conf. Thermoelectrics*, ICT'97, pp. 711–718.
[96] Goodson, K. E., and Ju, Y. S., 1999, ''Heat Conduction in Novel Electronic Films,'' Annu. Rev. Mater. Sci., **29**, pp. 261–293.
[97] Yang, B., Liu, J. L., Wang, K. L., and Chen, G., 2002, ''Simultaneous Measurements of Seebeck Coefficient and Thermal Conductivity Across Superlattices,'' Appl. Phys. Lett., in press.
[98] Fleurial, J.-P., Snyder, G. J., Herman, J. A., Giauque, P. H., et al. 1999, ''Thick-Film Thermoelectric Microdevices,'' *Proc. Int. Conf. Thermoelectrics*, ICT'99, pp. 294–300.
[99] Kishi, M., Yoshida, Y., Okano, H., Nemoto, H., Funanami, Y., Yamamoto, M., and Kanazawa, H., 1997, ''Fabrication of a Miniature Thermoelectric Module with Elements Composed of Sintered Bi-Te Compounds,'' *Proc. Int. Conf. Thermoelectrics*, ICT'97, pp. 653–656.
[100] Rushing, L., Shakouri, A., Abraham, P., and Bowers, J. E., 1997, ''Micro Thermoelectric Coolers for Integrated Applications,'' *Proc. Int. Conf. Thermoelectrics*, ICT'97, pp. 646–649.
[101] Volklein, F., Blumers, M., and Schmitt, L., ''Thermoelectric Microsensors and Microactuators (MEMS) Fabricated by Thin Film Technology and Micromachining,'' *Proc. Int. Conf. Thermoelectrics*, ICT'99, pp. 285–293.
[102] Yao, D.-J., Kim, C.-J., and Chen, G., 2000, ''Design of Thermoelectric Thin Film Coolers,'' ASME HTD-Vol. 366-2, pp. 245–251.
[103] Dutta, N. K., Cella, T., Brown, R. L., and Huo, D. T. C., 1985, ''Monolithically Integrated Thermoelectric Controlled Laser Diode,'' Appl. Phys. Lett., **47**, pp. 222–224.
[104] Chen, G., 1996, ''Heat Transfer in Micro- and Nanoscale Photonic Devices,'' Annu. Rev. Heat Transfer, **7**, pp. 1–57.
[105] Piprek, J., Akulova, Y. A., Babic, D. I., Coldren, L. A., and Bowers, J. E., 1998, ''Minimum Temperature Sensitivity of 1.55 μm Vertical-Cavity Lasers at 30 nm Gain Offset,'' Appl. Phys. Lett., **72**, pp. 1814–1816.
[106] Berger, P. R., Dutta, N. K., Choquette, K. D., Hasnain, G., and Chand, N., 1991, ''Monolithically Peltier-Cooled Vertical-Cavity Surface-Emitting Lasers,'' Appl. Phys. Lett., **59**, pp. 117–119.
[107] Corser, T. A., 1991, ''Qualification and Reliability of Thermoelectric Coolers for Use in Laser Modules,'' 41st Electronic Components and Technology Conference, Atlanta, GA, USA, May, pp. 150–156.
[108] Cheng, Y.-K., Tsai, C.-H., Teng, C.-C., and Kang, S.-M., 2000, *Electrothermal Analysis of VLSI Systems*, Kluwer Academic Publishers.
[109] Kishi, M., Nemoto, H., Hamao, T., Yamamoto, M., Sudou, S., Mandai, M., and Yamamoto, S., 1999, ''Micro Thermoelectric Modules and Their Application to Wristwatches as an Energy Source,'' *Proc. Int. Conf. Thermoelectrics*, ICT'99, pp. 301–307.